**Atmospheric
Chemistry
and Physics
Discussions**

Spectral dependence of aerosol light absorption over the Amazon Basin

L. V. Rizzo[1], A. L. Correia[2], P. Artaxo[2], A. S. Procópio[3], and M. O. Andreae[4]

[1]Institute of Environmental, Chemical and Pharmaceutics Sciences, Department of Earth and Exact Sciences, Federal University of São Paulo, Brazil
[2]Institute of Physics, University of São Paulo, Brazil
[3]Department of Sanitary and Environmental Engineering, Federal University of Juiz de Fora, Juiz de Fora, Brazil
[4]Max Planck Institute for Chemistry, Biogeochemistry Department, Mainz, Germany

Correspondence to: L. V. Rizzo (luvarizzo@gmail.com)

**Spectral dependence
of aerosol light
absorption over the
Amazon Basin**

L. V. Rizzo et al.

Title Page	
Abstract	Introduction
Conclusions	References
Tables	Figures
◄◄	►►
◄	►
Back	Close
Full Screen / Esc	
Printer-friendly Version	
Interactive Discussion	

Abstract

In this study, we examine the spectral dependence of aerosol absorption at different sites and seasons in the Amazon Basin. The analysis is based on measurements performed during three intensive field experiments at a pasture site (Fazenda Nossa Senhora, Rondônia) and at a primary forest site (Cuieiras Reserve, Amazonas), from 1999 to 2004. Aerosol absorption spectra were measured using two Aethalometers: a 7-wavelength Aethalometer (AE30) that covers the visible (VIS) to near-infrared (NIR) spectral range, and a 2-wavelength Aethalometer (AE20) that measures absorption in the UV and in the visible. As a consequence of biomass burning emissions, about 10 times greater absorption values were observed in the dry season in comparison to the wet season. Power law expressions were fitted to the measurements in order to derive the Ångström exponent for absorption, defined as the negative slope of absorption vs. wavelength in a log-log plot. At the pasture site, about 70% of the Ångström exponents fell between 1.5 and 2.5 during the dry season, indicating that biomass burning aerosols have a stronger spectral dependence than soot carbon particles. Ångström exponents decreased from the dry to the wet season, in agreement with the shift from biomass burning aerosols, predominant in the fine mode, to biogenic and dust aerosols, predominant in the coarse mode. The lowest Ångström exponents (90% of data below 1.5) were observed at the forest site during the dry season. Also, results indicate that low absorption coefficients were associated with Ångström exponents below 1.0. This finding suggests that biogenic aerosols from Amazonia may have a weak spectral dependence for absorption, contradicting our expectations of biogenic particles behaving as brown carbon. Nevertheless, additional measurements should be taken in the future, to provide a complete picture of biogenic aerosol absorption spectral characteristics from different seasons and geographic locations. The assumption that soot spectral properties represent all ambient light absorbing particles may cause a misjudgment of absorption towards the UV, especially in remote areas. Therefore, it is recommended to measure aerosol absorption at several wavelengths from UV to near

IR to accurately assess the impact of non-soot aerosols on climate and on photochemical atmospheric processes.

1 Introduction

Aerosols directly influence the Earth's energy budget by scattering and absorbing solar radiation. Aerosol light absorption affects the atmosphere by reducing the radiation reaching the surface. Furthermore, it can influence the tropospheric temperature structure, which in turn may have an effect on cloud formation, a phenomenon that has been called the semi-direct effect (Hansen et al., 1997). Also, aerosol absorption in the UV may affect atmospheric photolysis rates, influencing, for example, ozone concentrations in the troposphere (Albuquerque et al., 2005; Jacobson, 1999). In spite of the efforts to improve measurements and datasets over recent years, large uncertainties remain in the current estimates of aerosol forcing on climate, in part due to incomplete knowledge of aerosol absorption properties (Yu et al., 2006; IPCC, 2007).

Several studies have shown that the aerosol absorption coefficient decreases monotonically with wavelength (e.g., Bergstrom et al., 2007). It is usual to approximate this wavelength dependence by a power-law expression, taking the logarithm of absorption as a function of the logarithm of the wavelength. Often, a "linear" fit to this log-log curve is a good approximation:

$$\ln\left[\frac{\sigma_{abs}(\lambda)}{M\,m^{-1}}\right] = \ln(b) - \mathring{a}_{abs}\ln\left[\frac{\lambda}{nm}\right],\tag{1}$$

where $\sigma_{abs}(\lambda)$ is the absorption coefficient measured at the wavelength λ, $\mathring{a}_{abs}$ is known as the Ångström exponent for absorption, and b is known as the turbidity coefficient (Shuster et al., 2006). According to the original formulation by Ångström (1929), the fitting parameter $\mathring{a}_{abs}$ does not depend on wavelength. However, in some cases $\mathring{a}_{abs}$ shows a significant variation depending on the selected spectral range, requiring the

application of a "quadratic" fit:

$$\ln\left[\frac{\sigma_{abs}(\lambda)}{M\,m^{-1}}\right] = \ln(b) - \mathring{a}_{abs}\ln\left[\frac{\lambda}{nm}\right] + c\ln^2\left[\frac{\lambda}{nm}\right], \tag{2}$$

in which c is known as the curvature term (Shuster et al., 2006). Alternatively, it is possible to assess the variability of $\mathring{a}_{abs}$ by calculating its value from neighboring spectrum points ($\sigma_{abs}(\lambda_1)$; $\sigma_{abs}(\lambda_2)$) all across the measured spectral range:

$$\mathring{a}_{abs} = -\frac{\ln\left(\frac{\sigma_{abs}(\lambda_1)}{\sigma_{abs}(\lambda_2)}\right)}{\ln\left(\frac{\lambda_1}{\lambda_2}\right)}. \tag{3}$$

The spectral dependence of absorption relies on aerosol physical and chemical properties. The major light-absorbing components of aerosols are carbonaceous substances and mineral dust. According to Andreae and Gelencsér (2006), soot carbon particles, formed during combustion processes, consist of aggregates of spherules made of graphene layers, being almost purely carbon. Due to its morphology and relatively constant refractive index, the absorption spectrum of soot carbon is expected to exhibit Ångström exponents of about 1.0 (Sun et al., 2007). Measurements taken at urban areas support this statement (e.g., Marley et al., 2009; Bond and Bergstrom, 2006; Schnaiter et al., 2003). Besides soot, there are other kinds of light-absorbing carbonaceous aerosols in the atmosphere, originated either from low temperature combustion or from processes like oxidation of biogenic materials and polymerization (Andreae and Crutzen, 1997). These light absorbing particles are often denominated "brown carbon", and include soil humics, humic-like substances and biogenic aerosols, among others (Andreae and Gelencsér, 2006; Sun et al., 2007). The absorption cross section of non-soot carbon increases very sharply with decreasing wavelength, resulting in Ångström exponents significantly greater than unity. Ångström exponents greater than 1.5 have also been observed in dust aerosol (Bergstrom et al., 2007; Alexander et al., 2008). Ångström exponents for mixed aerosols originated from combustion of lignite,

Spectral dependence of aerosol light absorption over the Amazon Basin

L. V. Rizzo et al.

⏮ ⏭

◀ ▶

Back Close

Full Screen / Esc

Printer-friendly Version

Interactive Discussion

hard coal and biomass range from 1.0 to 2.5 (Kirchstetter, 2004). Studies indicate that, if soot particles were removed from these samples, the Ångström exponent for the remaining material would be greater than 2.5 (Sun et al., 2007). In accordance with that, Hoffer et al. (2006) obtained absorption Ångström exponents in the range of 6.0–7.0 for humic-like substances (HULIS) isolated from the fine fraction of biomass burning aerosols in Amazonia.

The different spectral dependence of absorption by soot carbon and other light absorbing aerosols implies that caution should be taken when extrapolating absorption measured at one single wavelength over the entire solar spectrum. The widespread assumption that soot spectral properties represent all ambient light absorbing particles may underestimate the absorption of UV radiation, especially when the mass concentration of soot is relatively low in comparison to that of brown carbon and dust. Therefore, it is important to describe accurately the spectral dependence of representative types of ambient aerosols to assess the impact of light absorbing particles on the Earth's energy budget.

This paper presents a systematic analysis of aerosol absorption spectra measured during three different field campaigns in Amazonia. It provides a general description of the wavelength dependence of absorption both during the Amazonian wet season, when the aerosol population is dominated by particles of biogenic origin, and during the dry season, when there is a strong influence of biomass burning emissions. It is important to describe accurately the optical behavior of these particles in order to assess the impact of anthropogenic changes on the regional climate. Since the Amazon forest is located in a region of intense convective activity, the aerosols released there can be long-range transported, potentially resulting in climate effects that are globally relevant (Ramanathan and Carmichael, 2008; Freitas et al., 2005; Andreae et al., 2001).

2   Materials and methods

2.1   Field experiments

This study is based on measurements taken during three intensive field experiments at two Amazonian sites, from 1999 to 2004. The pasture site (Fazenda Nossa Senhora, Rondônia state, Brazil) is located in the southwestern margin of the Amazon Basin, in an area under the influence of vegetation fire emissions during the dry season. The forest site (Cuieiras Reserve, Amazonas state, Brazil) is in a nature preserve, but occasionally receives the influence of regional biomass burning pollution during the dry season. All experiments were taken under the scope of the LBA project (Large-scale Biosphere-Atmosphere experiment in Amazonia) (Avissar et al., 2002; Davidson and Artaxo, 2004). Measurement conditions during each field experiment are briefly described below.

1. Pasture Dry 1999 – LBA/EUSTACH (European Studies on Trace gases and Atmospheric Chemistry): this intensive field experiment was conducted at a pasture site (Fazenda Nossa Senhora – FNS, 10°45.73′ S, 62°21.45′ W, 315 m a.s.l.) in Western Amazonia, from 17 September to 26 October 1999. During the whole experiment, the site was heavily affected by biomass burning emissions. Aerosol attenuation was measured at a height of 2 m, using a 7-wavelength Aethalometer (AE-30) (λ = 450, 571, 590, 615, 660, 880, and 950 nm). The 571-nm channel was not included in the analysis due to its systematically low signal. The Aethalometer was operated under ambient conditions with a 10 µm cut-off diameter. More details about this field experiment can be found in Andreae et al. (2002) or Artaxo et al. (2002).

2. Pasture Dry to Wet 2002 – LBA/SMOCC (Smoke, Aerosols, Clouds, Rainfall and Climate): the ground-based component of this intensive field experiment was conducted at the FNS pasture site from 5 September to 14 November 2002. Three periods can be distinguished: the dry period heavily influenced by biomass burn-

Full Screen / Esc

Printer-friendly Version

Interactive Discussion

ing events (5 September–7 October); a transition period in which the biomass burning signature was significantly reduced (8–30 October); and the wet period when the aerosol concentration reached its lowest levels (31 October–14 November) (Fuzzi et al., 2007). Aerosol attenuation was measured at a height of 2 m, using a 7-wavelength Aethalometer (AE-30) (λ = 450, 571, 590, 615, 660, 880, and 950 nm). The 571-nm and 590-nm channels were not included in the analysis due to systematically low signals. The Aethalometer was operated under ambient conditions with a 10 µm cut-off diameter. More details about this field experiment can be found in Andreae et al. (2004).

3. Forest Dry 2004 – LBA/ZF2-C14 Tower: this intensive field experiment was conducted at a forest site, Reserva do Cuieiras, located about 60 km NNW of Manaus. The experiment ran during the dry season, from 13 August to 1 October 2004 at the C14 tower ($2°35.35'$ S, $60°06.89'$ W, 140 m a.s.l.), located at km 14 of the ZF2 access road in the Cuieiras ecological reserve. The site is undisturbed by local biomass burning emissions. Nevertheless, during the dry season the site suffers the influence of biomass burning emissions through regional transport of air masses. Aerosol attenuation was measured above the canopy top (about 28 m), at a height of 40 m, using a 2-wavelength Aethalometer (AE-20) (370, 880 nm). The Aethalometer was operated under ambient conditions with a 10 µm cut-off diameter. More details about this field experiment can be found in Rizzo et al. (2010).

2.2 Aerosol attenuation measurements

Aethalometers measure the light attenuation through a quartz filter matrix as aerosols are deposited. The attenuation coefficient (σ_{ATN}) is given by

$$\sigma_{ATN} = \frac{A_f}{Q} \frac{\Delta ATN}{\Delta t}, \tag{4}$$

where A_f is the filter spot area, Q the volumetric flow rate and σATN is the change in attenuation during the time interval Δt. The standard output of the manufacturer provides equivalent black carbon mass concentration BC_{ATN} (ng m^{-3}), which is calculated from σ_{ATN} according to

$$BC_{ATN} = \frac{\sigma_{ATN}}{\alpha_{ATN}}, \tag{5}$$

where

$$\alpha_{ATN}\left[m^2\,g^{-1}\right] = \frac{14625}{\lambda\,[nm]} \tag{6}$$

is the spectral mass-specific attenuation cross-section based on a calibration using a solvent-based thermal desorption method for elemental carbon analysis. Aiming to minimize uncertainties (Schmid et al., 2001), the primary measurement parameter of the Aethalometer, σ_{ATN}, will be investigated in this study. Therefore, all BC_{ATN} values delivered by the manufacturer's data acquisition software were converted into σ_{ATN} using Eqs. (4) to (2.5).

2.3 Inferring absorption coefficients from attenuation measurements

Several studies report that the attenuation coefficient (σ_{ATN}) may differ significantly from the aerosol absorption coefficient, σ_{abs} (e.g., Weingartner et al., 2003; Arnott et al., 2005; Schmid et al., 2006; Moosmüller et al., 2009, 2011). The need to deposit the aerosol on a filter substrate during the measurement results in artifacts related to multiple scattering effects within the filter matrix, as well as filter loading effects. Weingartner et al. (2003) proposed the following correction to obtain absorption coefficients from Aethalometer attenuation measurements:

$$\sigma_{abs} = \sigma_{ATN}\frac{1}{C \cdot R(ATN)}, \tag{7}$$

where C (≥ 1) accounts for multiple light scattering effects within the filter and R(ATN) (≤ 1) corrects for filter loading effects. Due to aerosol-filter interactions, Aethalometers require site-specific calibration factors. The filter loading correction depends on attenuation, directly measured by the Aethalometer, to account for the decrease in sensitivity as the filter gets loaded with particles, and can be calculated through an empirical relationship:

$$R(\text{ATN}) = \left(\frac{1}{f} - 1\right)\frac{\ln \text{ATN} - \ln 10}{\ln 50 - \ln 10} + 1. \tag{8}$$

The parameter f is known as the shadowing factor, and depends on the type of the aerosol. Schmid et al. (2006) obtained $f = 1.2$ through an intercomparison of Aethalometer and PAS (photo acoustic spectrometer) measurements during the LBA/SMOCC experiment. They report that the loading effect accounts for a maximum sensitivity reduction of about 20% at 532 nm.

According to Schmid et al. (2006), the multiple scattering correction (C) is by far the most important effect when inferring absorption coefficients from attenuation. Its average value for the SMOCC dry and transition periods was determined as $C_{532} = 5.23 \pm 0.17$ at the reference wavelength of 532 nm. For the wet season, it was impossible to obtain calibration factors, mainly due to the poor signal-to-noise ratio caused by low aerosol loadings. The spectral dependence of C can be calculated using

$$C(\lambda) = C^*(\lambda) + m_s(\lambda)\frac{\omega_0(\lambda)}{1 - \omega_0(\lambda)}, \tag{9}$$

where m_s represents the fraction of the aerosol scattering coefficient that is erroneously interpreted as absorption, C^* is the multiple scattering correction factor that includes the effects of aerosol scattering, ω_0 is the aerosol single scattering albedo, and λ is the wavelength in nm. The parameters m_s and C^* are provided by Arnott et al. (2005). $\omega_0(\lambda)$ can be calculated assuming that the spectral dependence of aerosol scattering (σ_{scat}) and absorption (σ_{abs}) coefficients can be described by power-law relationships,

Full Screen / Esc

Printer-friendly Version

Interactive Discussion

with $\mathring{a}_{\text{scat}}$ and $\mathring{a}_{\text{abs}}$ being the respective Ångstrom exponents:

$$\varpi_0(\lambda) = \frac{\sigma_{\text{scat}}}{\sigma_{\text{scat}} + \sigma_{\text{abs}}} = \frac{\varpi_0(\lambda_{\text{ref}}) \cdot \left[\dfrac{\lambda}{\lambda_{\text{ref}}}\right]^{-\mathring{a}_{\text{scat}}}}{\varpi_0(\lambda_{\text{ref}}) \cdot \left[\dfrac{\lambda}{\lambda_{\text{ref}}}\right]^{-\mathring{a}_{\text{scat}}} + \left[1 - \varpi_0(\lambda_{\text{ref}})\right] \cdot \left[\dfrac{\lambda}{\lambda_{\text{ref}}}\right]^{-\mathring{a}_{\text{abs}}}} \tag{10}$$

Therefore, the spectral dependence of the correction factor C depends on the previous knowledge of ϖ_0 at some reference wavelength, as well as on the spectral dependence of aerosol scattering ($\mathring{a}_{\text{scat}}$) and absorption ($\mathring{a}_{\text{abs}}$) itself. Unfortunately, aerosol scatter-
ing coefficients at multiple wavelengths were not measured during any of the three experiments analyzed here. Thus, for lack of better choices, average values will be used, following the procedure from Schmid et al. (2006). The errors associated with the use of averages instead of specific values of ϖ_0 and $\mathring{a}_{\text{scat}}$ will be discussed in Sect. 2.4.
For the SMOCC experiment, Chand et al. (2006) reported average albedo values of 0.92 ± 0.02 at 545 nm, and average scattering Ångstrom exponents of 2.0 ± 0.4. Using these average values, $C(\lambda)$ now depends only on $\mathring{a}_{\text{abs}}$. This is an awkward situation, since $\mathring{a}_{\text{abs}}$ is actually what we want to determine, and it depends on itself. Schmid et al. (2006) solved this impasse by choosing a reasonable range of Ångstrom exponents for absorption ($\mathring{a}_{\text{abs}} = 1.0$, 1.5 and 2.0) and parameterizing C as a function of λ and $\mathring{a}_{\text{abs}}$:

$$C(\lambda) = C_{\text{ref}} \cdot \frac{\lambda^{A\ln(\lambda/\text{nm})+B}}{\lambda_{\text{ref}}^{A\ln(\lambda_{\text{ref}}/\text{nm})+B}}, \tag{11}$$

where $C_{\text{ref}} = C_{532}$, $\lambda_{\text{ref}} = 532$ nm, and the coefficients A and B are expressed as a function of $\mathring{a}_{\text{abs}}$:

$$\begin{aligned} A &= 0.102\mathring{a}_{\text{abs}}^2 - 0.187\mathring{a}_{\text{abs}} - 0.141 \\ B &= -1.275\mathring{a}_{\text{abs}}^2 + 2.564\mathring{a}_{\text{abs}} + 1.827 \end{aligned} \tag{12}$$

Using Eqs. (11) and (12) it is possible to derive the spectral dependence of the multiple scattering correction factor as a function of $\mathring{a}_{abs}$, specifically for the SMOCC experiment conditions ($\varpi_{0\,ref} = 0.92$ and $\mathring{a}_{scat} = 2.0$). However, since $\mathring{a}_{abs}$ is not known, an iterative procedure can be used, comprising the following steps:

5   1. As a first guess, use the spectral dependence of measured attenuation, i.e., the Ångstrom exponent for attenuation ($\mathring{a}_{ATN}$), to calculate $C(\lambda)$ from Eqs. (11) and (12).

   2. Determine absorption coefficients (σ_{abs}) using Eqs. (7), (8) and (11).

   3. Calculate a better estimative for $\mathring{a}_{abs}$ based on step II.

10   4. Repeat steps II and III until $\mathring{a}_{abs}$ converges with a precision of 0.005.

A similar procedure had been applied by Schmid et al. (2006) to their average attenuation spectrum. In the present work, the above procedure was applied for each measured attenuation spectrum, obtaining the best feasible determinations for $\mathring{a}_{abs}$ and σ_{abs}. With this iterative method, $\mathring{a}_{abs}$ converged in less than 6 iterations for the dataset 15 analyzed here. Overall, the corrected absorption coefficients at 450 nm were approximately 75% lower than the corresponding raw attenuation coefficients. Ångstrom exponents for absorption were roughly 40% greater than the corresponding Ångstrom exponents for attenuation.

Schmid et al. (2006) concluded that there was no significant variation of the 20 Aethalometer correction factors between the sampling periods of the SMOCC experiment (dry and transition). For lack of a better alternative, they recommended to apply the correction factors derived for the SMOCC dry and transition periods also to the data of the SMOCC wet period. Going even further than that, we applied the parameters A and B (Eq. 9) and the calibration factor C_{532} derived specifically for the 25 SMOCC data to another two experiments conducted in Amazonia: LBA/EUSTACH and LBA/ZF2-C14 (Sect. 2.1). The application of the SMOCC correction parameters to the LBA/EUSTACH data is reasonable, since the experiment was carried out at the

Spectral dependence of aerosol light absorption over the Amazon Basin

L. V. Rizzo et al.

same pasture site and same season. The main reason for applying the same correction parameters to the LBA/ZF2-C14 experiment, carried out at a forest site during the dry season, is the absence of reference absorption measurements, as well as of site-specific estimates of ω_0 and $\mathring{a}_{\text{scat}}$. The errors associated to an imprecise choice of ω_0

5 and $\mathring{a}_{\text{scat}}$ were evaluated through sensibility tests, to be discussed in the next section.

2.4 Potential errors associated with the calculation of absorption coefficients

Observations of ω_0 and $\mathring{a}_{\text{scat}}$ simultaneously with attenuation measurements were not available for the three experiments analyzed here. Therefore, average values had to be used to derive the spectral dependence of the multiple scattering correction factors,

10 ($C(\lambda)$): $\omega_0 = 0.92 \pm 0.02$ (545 nm) and $\mathring{a}_{\text{scat}} = 2.0 \pm 0.4$ (Chand et al., 2006). Errors associated with the use of averages instead of specific values were evaluated through sensibility tests.

A range of values of ω_0 (0.88 to 0.96) and $\mathring{a}_{\text{scat}}$ (1.2 to 2.8) was used to calculate $C(\lambda, \mathring{a}_{\text{abs}})$ through Eqs. (9) and (10). The correction factor C was then parameterized

15 as a function of $\mathring{a}_{\text{abs}}$ and λ, deriving new parameters A and B (similar to Eq. 12), in accordance with the method used by Schmid et al. (2006). Afterwards, the iteration procedure described in Sect. 2.3 was used to calculate σ_{abs} and $\mathring{a}_{\text{abs}}$, evaluating deviations for different combinations of ω_0 and $\mathring{a}_{\text{scat}}$.

Figure 1 shows the variability of σ_{abs} and $\mathring{a}_{\text{abs}}$ as a function of ω_0 and $\mathring{a}_{\text{scat}}$ for

20 two measured attenuation spectra, taken as examples. Both spectra were measured in the transition period, having attenuation coefficients (σ_{ATN}) at 450 nm of 102 and 179 M m^{-1}, respectively, and attenuation Ångstrom exponents ($\mathring{a}_{\text{ATN}}$) of 1.72 and 1.04, correspondingly. As $\mathring{a}_{\text{scat}}$ increases, the calculated σ_{abs} and $\mathring{a}_{\text{abs}}$ decrease. Assuming the average value $\mathring{a}_{\text{scat}} = 2.0$ may cause a maximum deviation of $\pm 10\%$ on σ_{abs} and

25 $\pm 40\%$ on $\mathring{a}_{\text{abs}}$, in the worst case. The dependence of σ_{abs} and $\mathring{a}_{\text{abs}}$ on ω_0 can be approximately described by a second order polynomial, based on $\mathring{a}_{\text{scat}}$: as $\mathring{a}_{\text{scat}}$ increases, the quadratic term of this dependence decreases. It was observed that this quadratic term can reach negative values for spectra with $\mathring{a}_{\text{ATN}}$ lower than approximately 1.2, in

a way that σ_{abs} and $\mathring{a}_{abs}$ decrease with ω_0 (Fig. 1c,d). However, in most of the cases, σ_{abs} and $\mathring{a}_{abs}$ increase with ω_0. Assuming the average value $\omega_0 = 0.92$ may cause a maximum deviation of ±6% on σ_{abs} and ±25% on $\mathring{a}_{abs}$, in the worst case.

2.5 Data treatment

For a systematic analysis of the aerosol absorption spectral dependence in Amazonia, the linear fit (Eq. 1), the quadratic fit (Eq. 2) and the slope between neighboring points (Eq. 3) were computed for all corrected absorption spectra from the 7-wavelength Aethalometer (Pasture Dry 1999 and Pasture Dry to Wet 2002). As will be discussed below, in most of the cases the absolute value of the curvature term (c) was close to zero, so that the quadratic fit was roughly equivalent to the linear fit. For the spectra measured at two wavelengths (Forest Dry 2004), it was only possible to calculate the slope between 370 and 880 nm (Eq. 3).

Two criteria were used to filter the Aethalometer data sets to assure the quality of the measured spectra:

1. The adjusted R^2 of the quadratic fit should be greater than 0.85. Adjusted R^2 means the coefficient of determination (R^2) adjusted by the degree of freedom of the fitting. The reason for this criterion is that if a quadratic curve cannot fit satisfactorily a spectrum, it means that this particular measurement was too noisy and should not be considered as a valid observation. More than 95% of the spectra satisfied this criterion.

2. The measured attenuation should be above the detection limit of the instrument, considering its sampling time and flow. According to the Aethalometer manual, the detection limit of the instrument corresponds to a mass increase of 5 ng on the filter. This limit can be translated into $\mathrm{M\,m^{-1}}$ units using the following expression:

$$\min(\sigma_{abs}) = \frac{m \cdot \alpha_{ATN}(\lambda)}{\Delta t \cdot Q} \quad \left[\mathrm{M\,m^{-1}}\right], \tag{13}$$

where $m = 5$ ng, $\alpha_{\text{ATN}}(\lambda)$ is the specific absorption cross-section in m^2 g^{-1} (Eq.), Δt is the sampling time in minutes, and Q is the sampling flow in dm^3 min^{-1}.

Obviously, only the filter criterion II could be applied to the absorption spectra measured at two wavelengths.

5   Table 1 shows the calculated the Aethalometer detection limit for the different field studies considered here. It also shows the total number of observed attenuation spectra, as well as the percentage of spectra satisfying the criteria described above.

3   Results and discussion

Average absorption spectra calculated for the three field experiments are shown in
10 Fig. 2. The SMOCC campaign was divided into three periods, dry, transition and wet, as described before (Sect. 2.1). The averages included all spectra that fulfilled the filtering criteria mentioned in Sect. 2.5. As expected, greater absorption values were observed during the dry season, as a consequence of biomass burning emissions. Note the good agreement between Pasture Dry 1999 (EUSTACH) and Pasture Dry
15 2002 (SMOCC) curves, measured at the same pasture site within a period of three years. From the dry to the wet season, aerosol absorption at 450 nm decreased approximately by a factor of 10 at the pasture site. Absorption coefficients at the forest site during the dry season are intermediate in magnitude between the Pasture Dry and Pasture Wet curves. While there were no local fires at the forest site, the location was
20 influenced by regional biomass burning emissions carried along by air masses. An absorption spectrum with slope of −1, typical of soot aerosols, is represented in Fig. 1 by a dashed black line.

To assess the variability of the spectral dependence over the averages represented in Fig. 2, Ångström exponents were calculated for each absorption spectrum measured
25 during the three field campaigns, considering the filtering criteria stated in Sect. 2.3. Here will be discussed the variability of Ångström exponents calculated through a linear

Full Screen / Esc

Printer-friendly Version

Interactive Discussion

fit over the whole spectrum (Eq. 1) ($\mathring{a}_{abs}^{lin}$), and as the negative slope between two neighboring wavelength values (Eq. 3) ($\mathring{a}_{abs}^{450/615}$ and $\mathring{a}_{abs}^{370/880}$). Figure 3 shows histograms of $\mathring{a}_{abs}^{lin}$ for the three field campaigns.

At the pasture site, 60 to 70% percent of $\mathring{a}_{abs}^{lin}$ (Fig. 3a,b) fell between 1.5 and 2.5 during the dry season. This is in accordance with Kirchstetter et al. (2004), who reported absorption Ångström exponents of approximately 2.0 for biomass burning aerosols, as a result of enhanced light absorption at wavelengths shorter than 600 nm. The authors suggest that low-temperature and incomplete combustion processes, such as biomass burning, can produce absorbing aerosols with a stronger spectral dependence as compared to high-temperature combustion processes that generate soot.

Particularly during the SMOCC experiment, it was possible to observe a consistent decrease of the average absorption Ångström exponent as the weather regime moved from dry to wet season (Fig. 3b). Also, Fig. 4 shows that in the SMOCC experiment low absorption coefficients were associated with Ångström exponents below 1.0. That also holds for the other two experiments, indicating that the Amazonian natural aerosol population has a weaker absorption spectral dependence than combustion aerosols. Moosmüller et al. (2011) modeled the absorption spectra of homogeneous spherical brown carbon particles and found a decrease of Ångström exponents toward larger particle diameters (from 0.1 to 10 μm). Therefore, the decrease of Ångström exponents from dry to wet season is consistent with the shift from biomass burning aerosols, predominant in the fine mode, to biogenic and dust aerosols, predominant in the coarse mode. In addition to the effect of aerosol size, another possible explanation would be the rain scavenging of soluble organic aerosols during the wet season, resulting in an enrichment of insoluble soot carbon particles in the remaining aerosol. This effect could also shift the Ångström exponents to lower values from dry to wet season.

The lowest Ångström exponents were observed at the forest site in the dry season (LBA/ZF2-C14 experiment), with a mean value of $\mathring{a}_{abs}^{370/880} = 1.3 \pm 0.3$ (Fig. 3c). As this forest site is in a remote preserve, even during the dry season biogenic particles com-

Spectral dependence of aerosol light absorption over the Amazon Basin

L. V. Rizzo et al.

Title Page

Abstract	Introduction
Conclusions	References
Tables	Figures

⏮ ⏭

◀ ▶

Back Close

Full Screen / Esc

Printer-friendly Version

Interactive Discussion

prise the majority of the particulate matter (75%), while other light absorbing particles (soil dust and soot-like) account for 13% of the total aerosol mass (Rizzo et al., 2010). The fact that 90% of the observed Ångström exponents are below 1.5 suggests that Amazonian biological particles have a weak spectral dependence for absorption. This finding contradicts our expectations of biogenic particles behaving as "brown carbon", i.e., particles that show absorption coefficients sharply increasing at wavelengths below 600 nm. Nevertheless, additional measurements should be performed at forest sites in Amazonia to provide a complete picture of biogenic aerosol absorption spectral characteristics regarding different seasons and geographic locations.

Table 2 summarizes the average magnitude of aerosol absorption observed at each site and season considered in this study, which agrees with previously reported data (Artaxo et al., 2002; Schmid et al., 2006; Chand et al., 2006). It also shows the corresponding average Ångström exponents $\mathring{a}_{abs}^{lin}$, $\mathring{a}_{abs}^{450/615}$ and $\mathring{a}_{abs}^{370/880}$. Considering the standard deviations, the mean values of both $\mathring{a}_{abs}^{lin}$ and $\mathring{a}_{abs}^{450/615}$ are statistically compatible for all measurements taken at the pasture site. The percentage of spectra in which the linear fit was a good approximation (adjusted R^2 greater than 0.90), was above 94%, indicating that in most of the cases the Ångström exponent was approximately constant throughout the observed spectral region.

Figure 5 shows the cumulative histogram of Ångström exponents for the field studies in which the 7-wavelength Aethalometer was available. It indicates the variability of Ångström exponents as a function of wavelength. The spectral dependence between 450 and 615 nm can be up to 10% steeper than the Ångström exponent derived from the complete measured spectra (450–950 nm). Also, this 10% difference between $\mathring{a}_{abs}^{450/615}$ and $\mathring{a}_{abs}^{lin}$ does not justify the application of quadratic fits to the aerosol absorption spectra. The linear fit was a good approximation in more than 94% of the observed spectra (Table 2).

At the pasture site, Ångström exponents observed during the day were about 20% lower than at nighttime (Fig. 6). The diurnal cycle of absorption coefficients and aerosol

number concentration (not shown) follow a similar pattern, most likely a consequence of the dynamics of the boundary layer. Chand et al. (2006) reported higher albedo values for the SMOCC experiment during daytime, and argued that diurnal aerosols are more aged than the nocturnal ones. Aged smoke particles undergo a size increase
5 due to coagulation and condensation of inorganic and organic species, with impacts on aerosol optical properties (Reid et al., 1998). Accordingly, Rissler et al. (2006) observed higher aerosol modal diameters during daytime compared to nighttime for the SMOCC experiment. The decreased Ångström exponents for absorption observed at daytime might be either an outcome of increased particle sizes (Moosmüller et al.,
10 2011) or a consequence of the change in particle chemical composition due to the condensation of absorbing species with a weaker spectral dependence.

4   Summary and conclusions

The wavelength dependence of aerosol absorption in Amazonia was studied for different sites and seasons. As expected, greater absorption values were observed at
15 the pasture site during the dry season, as a consequence of biomass burning emissions, with average values around $30\,\mathrm{M\,m^{-1}}$ at 450 nm. At the onset of the wet season, aerosol absorption coefficients decreased by one order of magnitude (to $2.7\,\mathrm{M\,m^{-1}}$ at 450 nm on average). Absorption coefficients at the forest site during the dry season were intermediate in magnitude, falling between the observations taken during the dry
20 and wet seasons at the pasture site.

Ångström exponents for absorption did not vary significantly with wavelength, so that, in most cases, a power law fit could be applied over the whole measured spectral range (450–950 nm). About 70% of the a_{abs}^{lin} Ångström exponents observed at the pasture site during the dry season fell between 1.5 and 2.5, suggesting the presence of light-
25 absorbing organic carbon (brown carbon) released from biomass burning emissions. Average diurnal cycles of Ångström exponents for the pasture site showed a clear pattern, with values 20% lower at daytime, when the aerosol population is dominated by

larger and more aged particles (Chand et al., 2006; Rissler et al., 2006). The decreased Ångström exponents during the day might be either an outcome of increased particle sizes (Moosmüller et al., 2011) or a consequence of changes in particle chemical composition due to the condensation of absorbing species with a lesser spectral dependence.

At the pasture site, throughout the transition from dry to wet season, average Ångström exponents decreased, in agreement with the shift from biomass burning aerosols, predominant in the fine mode, to biogenic and dust aerosols, predominant in the coarse mode. Low Ångström exponents (below 1.5) were also observed in 90% of the absorption spectra measured at the forest site during the dry season. Results indicate that low absorption coefficients (below ca. $15\,\mathrm{M\,m^{-1}}$ at 450 nm), typically observed under unpolluted conditions in Amazonia, are associated with Ångström exponents below 1.0. This finding suggests that biogenic aerosols from Amazonia may have a weak spectral dependence for absorption, contradicting our expectations of biogenic particles behaving as brown carbon. Nevertheless, additional measurements should be taken in the future, to provide a complete picture of biogenic aerosol absorption spectral characteristics in different seasons and geographic locations.

Our results show that caution must be taken when extrapolating aerosol absorption measured at one single wavelength over the entire solar spectrum. The widespread assumption that soot spectral properties represent all ambient light absorbing particles may cause a underestimate of absorption in the UV spectral range. Especially in remote areas, it is advisable to measure aerosol absorption at several wavelengths from UV to near IR to accurately assess the impact of non-soot aerosols on climate and photochemical atmospheric processes. If measurements are taken using a filter-based attenuation method, it is advisable to have simultaneous observations of aerosol scattering at several wavelengths and a reference absorption measurement for proper calibration.

References

Albuquerque, L. M. M., Longo, K. M., Freitas, S. R., Tarasova, T., Plana Fattori, A., Nobre, C., and Gatti, L. V.: Sensitivity studies on the photolysis rates calculation in Amazonian atmospheric chemistry – Part I: The impact of the direct radiative effect of biomass burning aerosol particles, Atmos. Chem. Phys. Discuss., 5, 9325–9353, doi:10.5194/acpd-5-9325-2005, 2005.

Alexander, D. T. L., Crozier, P. A., and Anderson, J. R.: Brown carbon spheres in East Asian outflow and their optical properties, Science, 321, 833–836, 2008.

Andreae, M. O., Aerosols before pollution, Science, 315 (5808), 50–51, 2007.

Andreae, M. O. and Crutzen, P. J.: Atmospheric aerosols: biogeochemical sources and role in atmospheric chemistry, Science, 276, 1052–1056, 1997.

Andreae, M. O. and Gelencsér, A.: Black carbon or brown carbon? The nature of light-absorbing carbonaceous aerosols, Atmos. Chem. Phys., 6, 3131–3148, doi:10.5194/acp-6-3131-2006, 2006.

Andreae, M. O., Artaxo, P., Fischer, H., Freitas, S. R., Grégoire, J.-M., Hansel, A., Hoor, P., Kormann, R., Krejci, R., Lange, L., Lelieveld, J., Lindinger, W., Longo, K., Peters, W., de Reus, M., Scheeren, B., Silva Dias, M. A. F., Ström, J., van Velthoven, P. F. J., and Williams, J.: Transport of biomass burning smoke to the upper troposphere by deep convection in the equatorial region, Geophys. Res. Lett., 28, 951–954, doi:10.1029/2000GL012391, 2001.

Andreae, M. O., Artaxo, P., Brandão, C., Carswell, F. E., Ciccioli, P., da Costa, A. L., Culf, A. D., Esteves, J. L., Gash, J. H. C., Grace, J., Kabat, P., Lelieveld, J., Malhi, Y., Manzi, A. O., Meixner, F. X., Nobre, A. D., Nobre, C., Ruivo, M. D. L. P., Silva-Dias, M. A., Stefani, P., Valentini, R., von Jouanne, J., and Waterloo, M. J.: Biogeochemical cycling of carbon, water,

energy, trace gases, and aerosols in Amazonia: the LBA-EUSTACH experiments, J. Geophys. Res., 107 (D20), 8066, doi:10.1029/2001JD000524, 2002.

Andreae, M. O., Rosenfeld, D., Artaxo, P., Costa, A. A., Frank, G. P., Longo, K. M., and Silva-Dias, M. A. F.: Smoking rain clouds over the Amazon, Science, 303, 1337–1342, 2004.

5 Arnott, W. P., Hamasha, K., Moosmüller, H., Sheridan, P. J., and Ogren, J. A.: Towards aerosol light-absorption measurements with a 7-wavelength aethalometer: evaluation with a photoacoustic instrument and 3-wavelength nephelometer, Aerosol Sci. Technol., 39, 17–29, 2005.

Artaxo, P., Martins, J. V., Yamasoe, M. A., Procópio, A. S., Pauliquevis, T. M., Andreae, M. O., Guyon, P., Gatti, L. V., and Leal, A. M. C.: Physical and chemical properties of aerosols
10 in the wet and dry seasons in Rondônia, Amazonia, J. Geophys. Res., 107 (D20), 8081, doi:10.1029/2001JD000666, 2002.

Avissar, R., Silva Dias, P. L., Silva Dias, M. A. F., and Nobre, C.: The Large-Scale Biosphere-Atmosphere Experiment in Amazonia (LBA): Insights and future research needs. J. Geophys. Res., 107(D20), 8086, doi:10.1029/2002JD002704, 2002.

15 Bergstrom, R. W., Pilewskie, P., Russell, P. B., Redemann, J., Bond, T. C., Quinn, P. K., and Sierau, B.: Spectral absorption properties of atmospheric aerosols, Atmos. Chem. Phys., 7, 5937–5943, doi:10.5194/acp-7-5937-2007, 2007.

Bond, T. C.: Spectral dependence of visible light absorption by carbonaceous particles emitted from coal combustion, Geophys. Res. Lett., 28, 4075–4078, 2001.

20 Chand, D., Guyon, P., Artaxo, P., Schmid, O., Frank, G. P., Rizzo, L. V., Mayol-Bracero, O. L., Gatti, L. V., and Andreae, M. O.: Optical and physical properties of aerosols in the boundary layer and free troposphere over the Amazon Basin during the biomass burning season, Atmos. Chem. Phys., 6, 2911–2925, doi:10.5194/acp-6-2911-2006, 2006.

Davidson, E. A. and Artaxo, P.: Globally significant changes in biological processes of the
25 Amazon Basin: results of the large-scale biosphere-atmosphere experiment, Glob. Change Biol., 10(5), 1–11, doi:10.1111/j.1529-8817.2003.00779, 2004.

Freitas, S. R., Longo, K. M., Silva Dias, M. A. F., Silva Dias, P. L., Chatfield, R., Prins, E., Artaxo, P., Grell, G. A., and Recuero, F. S.: Monitoring the transport of biomass-burning emissions in South America, Environ. Fluid Mech., 5, 135–167, doi:10.1007/s10652-005-
30 0243-7, 2005.

Fuzzi, S., Decesari, S., Facchini, M. C., Cavalli, F., Emblico, L., Mircea, M., Andreae, M. O., Trebs, I., Hoffer, A., Guyon, P., Artaxo, P., Rizzo, L. V., Lara, L. L., Pauliquevis, T., Maenhaut, W., Raes, N., Chi, X., Mayol-Bracero, O. L., Soto-García, L. L., Clayes, M., Kourtchev, I.,

Spectral dependence of aerosol light absorption over the Amazon Basin

L. V. Rizzo et al.

Rissler, J., Swietlicki, E., Tagliavini, E., Schkolnik, G., Falkovich, A. H., Rudich, Y., Fisch, G., and Gatti, L. V.: Overview of the inorganic and organic composition of size-segregated aerosol in Rondônia, Brazil, from the biomass burning period to the onset of the wet season, J. Geophys. Res., 112, D01201, doi:10.1029/2005JD006741, 2007.

5 Grahan, B., Guyon, P., Maenhaut, W., Taylor, P., Ebert, M., Maser, S. M., Mayol Bracero, O. L., Godoy, R., Meixner, F. X., and Artaxo, P.: Composition and diurnal variations of the natural Amazonian aerosol, J. Geophys. Res., 108(D24), 4765, 2003.

Guyon, P., Graham, B., Beck, J., Boucher, O., Gerasopoulos, E., Mayol-Bracero, O. L., Roberts, G. C., Artaxo, P., and Andreae, M. O.: Physical properties and concentration of

10 aerosol particles over the Amazon tropical forest during background and biomass burning conditions, Atmos. Chem. Phys., 3, 951–967, doi:10.5194/acp-3-951-2003, 2003.

Hansen, J., Sato, M., and Ruedy, R.: Radiative forcing and climate response, J. Geophys. Res., 102, 6831–6864, 1997.

Hoffer, A., Gelencsér, A., Guyon, P., Kiss, G., Schmid, O., Frank, G. P., Artaxo, P., and

15 Andreae, M. O.: Optical properties of humic-like substances (HULIS) in biomass-burning aerosols, Atmos. Chem. Phys., 6, 3563–3570, doi:10.5194/acp-6-3563-2006, 2006.

IPCC, Climate Change 2007: The Physical Science Basis. Contribution of Working Group I to the Fourth Assessment Report of the Intergovernmental Panel on Climate Change, edited by: Solomon, S., Qin, D., Manning, M., Chen, Z., Marquis, M., Averyt, K., Tignor, M., and

20 Miller, H. L., Cambridge University Press, Cambridge and New York, 996 pp., 2007.

Jacobson, M. Z.: Isolation nitrated and aromatic aerosols and nitrated aromatic gases as sources of ultraviolet light absorption, J. Geophys. Res., 104, 3527–3542, 1999.

Kirchstetter, T. W., Novakov, T., and Hobbs, P. V.: Evidence that the spectral dependence of light absorption by aerosols is affected by organic carbon, J. Geophys. Res., 109, D21208,

25 doi:10.1029/2004JD004999, 2004.

Marley, N. A., Gaffney, J. S., Castro, T., Salcido, A., and Frederick, J.: Measurements of aerosol absorption and scattering in the Mexico City Metropolitan Area during the MILAGRO field campaign: a comparison of results from the T0 and T1 sites, Atmos. Chem. Phys., 9, 189–206, doi:10.5194/acp-9-189-2009, 2009.

30 Moosmüller, H., Chakrabarty, R. K., and Arnott, W. P.: Aerosol light absorption and its measurement: a review, J. Quant. Spectrosc. Ra., 110(11), 844–878, doi:10.1016/j.jqsrt.2009.02.035, 2009.

Moosmüller, H., Chakrabarty, R. K., Ehlers, K. M., and Arnott, W. P.: Absorption Ångström

Spectral dependence of aerosol light absorption over the Amazon Basin

L. V. Rizzo et al.

Title Page

Abstract	Introduction
Conclusions	References
Tables	Figures

|◄ | ►|

◄ | ►

Back | Close

Full Screen / Esc

Printer-friendly Version

Interactive Discussion

coefficient, brown carbon, and aerosols: basic concepts, bulk matter, and spherical particles, Atmos. Chem. Phys., 11, 1217–1225, doi:10.5194/acp-11-1217-2011, 2011.

Müller, T., Henzing, J. S., de Leeuw, G., Wiedensohler, A., Alastuey, A., Angelov, H., Bizjak, M., Collaud Coen, M., Engström, J. E., Gruening, C., Hillamo, R., Hoffer, A., Imre, K., Ivanow, P., Jennings, G., Sun, J. Y., Kalivitis, N., Karlsson, H., Komppula, M., Laj, P., Li, S.-M., Lunder, C., Marinoni, A., Martins dos Santos, S., Moerman, M., Nowak, A., Ogren, J. A., Petzold, A., Pichon, J. M., Rodriquez, S., Sharma, S., Sheridan, P. J., Teinilä, K., Tuch, T., Viana, M., Virkkula, A., Weingartner, E., Wilhelm, R., and Wang, Y. Q.: Characterization and intercomparison of aerosol absorption photometers: result of two intercomparison workshops, Atmos. Meas. Tech., 4, 245–268, doi:10.5194/amt-4-245-2011, 2011.

Ramanathan, V. and Carmichael, G.: Global and regional climate changes due to black carbon, Nature Geosci., 1, 221–227, 2008.

Reid, J. S., Hobbs, P. V., Ferek, R. J., Blake, D. R., Martins, J. V., Dunlap, M. R., and Liousse C.: Physical, chemical and optical properties of regional hazes dominated by smoke in Brazil, J. Geophys. Res., 103, 32059–32080, 1998.

Rissler, J., Vestin, A., Swietlicki, E., Fisch, G., Zhou, J., Artaxo, P., and Andreae, M. O.: Size distribution and hygroscopic properties of aerosol particles from dry-season biomass burning in Amazonia, Atmos. Chem. Phys., 6, 471–491, doi:10.5194/acp-6-471-2006, 2006.

Rizzo, L. V., Artaxo, P., Karl, T., Guenther, A. B., and Greenberg, J.: Aerosol properties, in-canopy gradients, trubulent fluxes and VOC concdntrations at a pristine forest site in Amazonia, Atmos. Env., 44, 503–511, 2010.

Schmid, H., Laskus, L., Abraham, H. J., Baltensperger, U., Lavanchy, V., Bizjak, M., Burba, P., Cachier, H., Crow, D., Chow, J., Gnauk, T., Even, A., Brink, H. M., Giesen, K.-P., Hitzenberger, R., Hueglin, C., Maenhaut, W., Pio, C., Carvalho, A., Putaud, J.-P., Toom-Sauntry, D., and Puxbaum, H.: Results of the "carbon conference" international aerosol carbon round robin test stage I, Atmos. Env., 35(12), 2111–2121, doi:10.1016/S1352-2310(00)00493-3, 2001.

Schmid, O., Artaxo, P., Arnott, W. P., Chand, D., Gatti, L. V., Frank, G. P., Hoffer, A., Schnaiter, M., and Andreae, M. O.: Spectral light absorption by ambient aerosols influenced by biomass burning in the Amazon Basin. I: Comparison and field calibration of absorption measurement techniques, Atmos. Chem. Phys., 6, 3443–3462, doi:10.5194/acp-6-3443-2006, 2006.

Schnaiter, M., Horvath, H., Möhler, O., Naumann, K. H., Saathoff, H., and Schöck, O. W.: UV-

VIS-NIR spectral optical properties of soot and soot-containing aerosols, J. Aerosol Sci., 34, 1421–1444, 2003.

Schuster, G. L., Dubovick, O., and Holben, B. N.: Ångström exponent and bimodal aerosol size distributions, J. Geophys. Res., 111, D07207, doi:10.1029/2005/JD006328, 2006.

Sun, H., Biedermann, L., and Bond, T. C.: Color of brown carbon: a model for ultraviolet and visible light absorption by organic carbon aerosol, Geophys. Res. Lett., 34, L17813, doi:10.1029/2007GL029797, 2007.

Weingartner, E., Saathoff, H., Schnaiter, M., Streit, N., Bitnar, B., and Baltensperger, U.: Absorption of light by soot particles: determination of the absorption coefficient by means of aethalometers, J. Aerosol Sci., 34, 1445–1463, 2003.

Yamasoe, M. A., Artaxo, P., Miguel, A. H., and Allen, A. G.: Chemical composition of aerosol particles from direct emissions of vegetation fires in the Amazon Basin: water-soluble species and trace elements, Atmos. Env., 34, 1641–1653, 2000.

Yu, H., Kaufman, Y. J., Chin, M., Feingold, G., Remer, L. A., Anderson, T. L., Balkanski, Y., Bellouin, N., Boucher, O., Christopher, S., DeCola, P., Kahn, R., Koch, D., Loeb, N., Reddy, M. S., Schulz, M., Takemura, T., and Zhou, M.: A review of measurement-based assessments of the aerosol direct radiative effect and forcing, Atmos. Chem. Phys., 6, 613–666, doi:10.5194/acp-6-613-2006, 2006.

Table 1. For all the field experiments considered in this analysis, this table shows: measurement period; Aethalometer sampling time; calculated detection limit at 450 nm; total number of measured attenuation spectra; percentage of spectra satisfying the filtering criteria described in the text.

Experiment	Measurement period	Sampling time (min)	Detection limit at 450 nm ($M m^{-1}$)	Number of measured spectra	Percent of spectra satisfying the filtering criteria
Forest Dry 2004 LBA/ZF2-C14	13 Aug–1 Oct 2004	5	10.0[*]	9618	90%
Pasture Dry to Wet 2002 LBA/SMOCC	5 Sep–14 Nov 2002	15	2.0	5840	90%
Pasture Dry 1999 LBA/EUSTACH	17 Sep–26 Oct 1999	10	2.0	4684	91%

[*] Detection limit at 370 nm.

Table 2. Average absorption coefficient measured for each field experiment, as well as average Ångström exponents calculated through linear fit ($\mathring{a}_{abs}^{lin}$), through the slope between 450 and 615 nm ($\mathring{a}_{abs}^{450/615}$) and between 370 and 880 nm ($\mathring{a}_{abs}^{370/880}$). Also shown the percentage of spectra in which the linear fit was a good approximation (adjusted $R^2 > 0.90$).

Experiment	σ_{abs} (450) $M\,m^{-1}$	Ångström linear fit ($\mathring{a}_{lin}$)	Ångström 450/615 nm ($\mathring{a}_{450/615}$)	Percent of spectra with good linear fit
Forest Dry 2004 (ZF2-C14)	$11 \pm 8^{*}$	$1.3 \pm 0.3^{**}$	–	–
Pasture 2002 (SMOCC)	21 ± 22	1.7 ± 0.4	1.8 ± 0.6	99%
Pasture Dry 2002 (SMOCC)	33 ± 25	1.8 ± 0.4	1.9 ± 0.5	100%
Pasture Transition 2002 (SMOCC)	11 ± 7	1.6 ± 0.4	1.7 ± 0.5	99%
Pasture Wet 2002 (SMOCC)	2.7 ± 2.2	1.5 ± 0.4	1.6 ± 0.7	95%
Pasture Dry 1999 (EUSTACH)	26 ± 21	1.7 ± 0.4	1.9 ± 0.6	94%

[*] Absorption at 370 nm.

[**] Equivalent to $\mathring{a}_{abs}^{370/880}$.
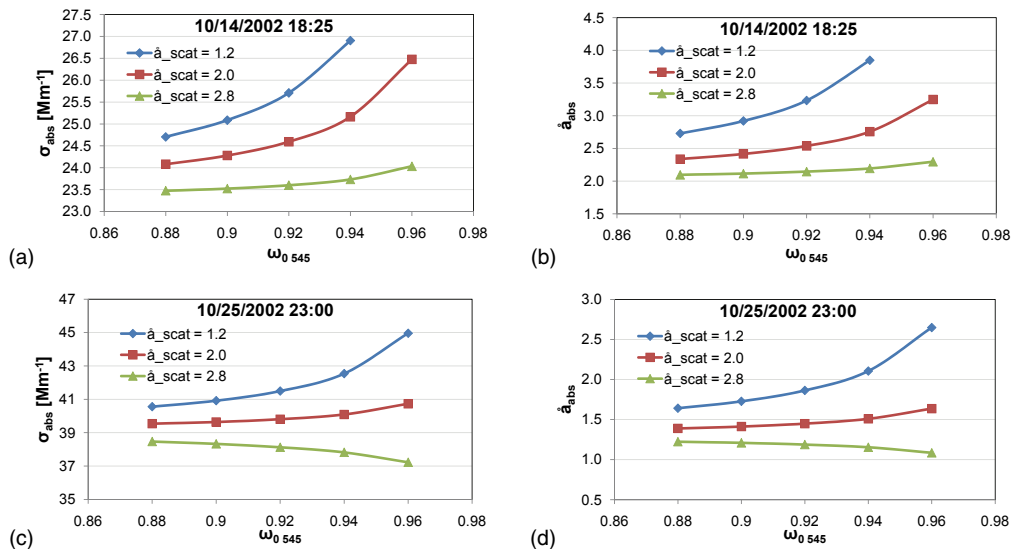
Fig. 1. Dependence of calculated σ_{abs} and $\mathring{a}_{abs}$ on ω_0 and $\mathring{a}_{scat}$ for two measured attenuation spectra measured during the LBA/SMOCC experiment: **(a, b)** 14 October 2002 18:25 LT; **(c, d)** 25 October 2002 23:00 LT. The measured spectra had attenuation coefficients (σ_{ATN}) at 450 nm of 102 and 179 M m^{-1}, respectively, and attenuation Ångstrom exponents ($\mathring{a}_{ATN}$) of 1.72 and 1.04, correspondingly.
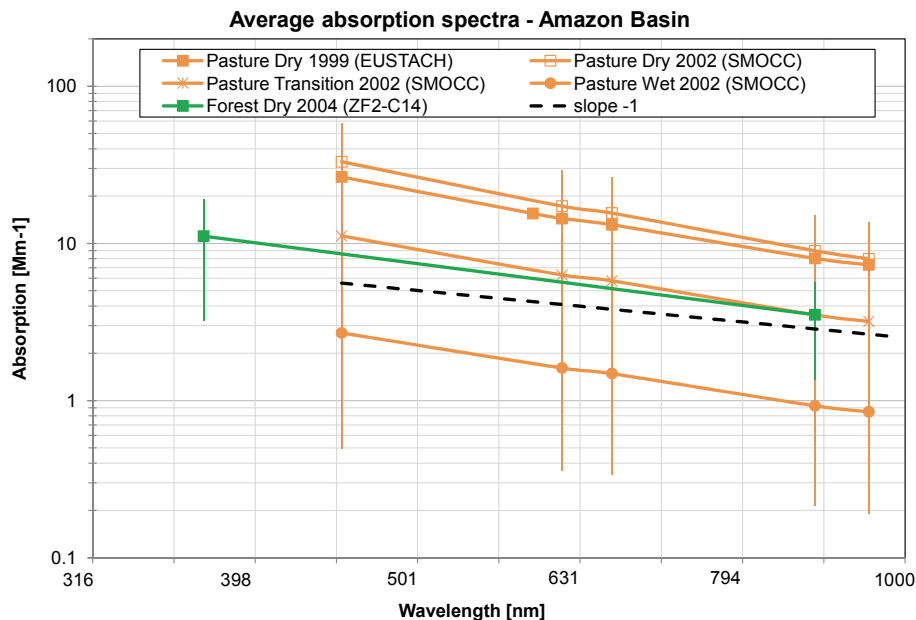
Fig. 2. Average aerosol absorption spectra for: Pasture Dry 1999 (EUSTACH) – comprising 4265 spectra; Pasture Dry to Wet 2002 (SMOCC) – comprising 5296 spectra; Forest Dry 2004 (ZF2-C14) – comprising 7927 spectra. Error bars represent statistical standard deviations. Also shown is a spectrum with a slope of −1, characteristic of soot aerosol (black dashed line).
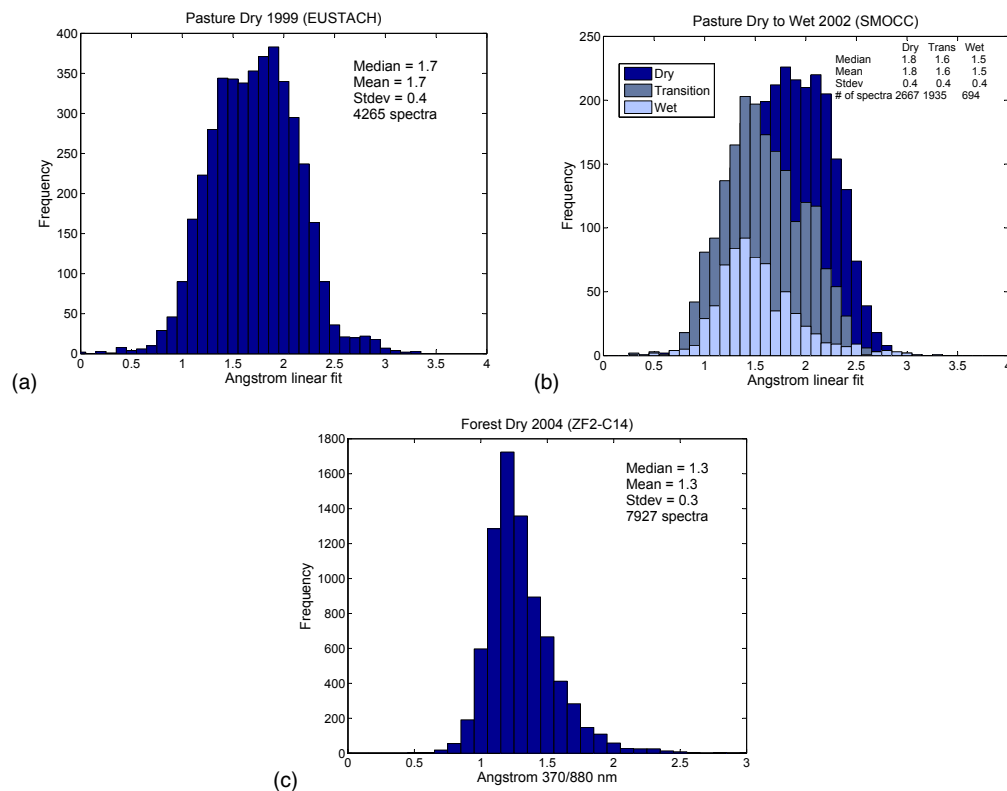
Fig. 3. Histograms of absorption Ångström exponents for the field experiments: **(a)** Pasture Dry 1999 (LBA/EUSTACH); **(b)** Pasture Dry to Wet 2002 (LBA/SMOCC); **(c)** Forest Dry 2004 (LBA/ZF2-C14).
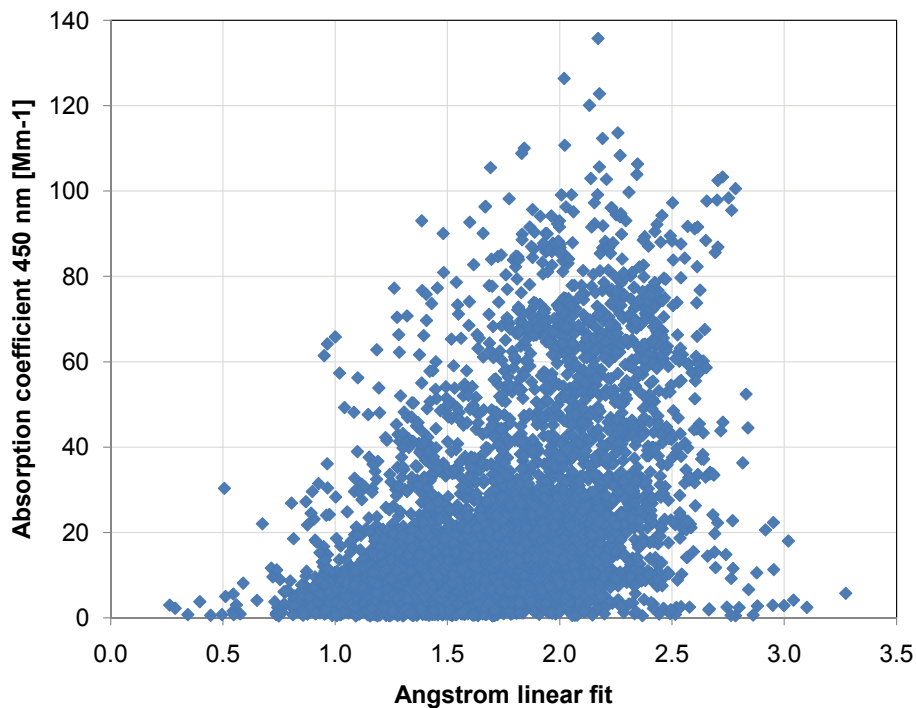
Fig. 4. Aerosol absorption coefficients at 450 nm vs. Ångström exponents calculated through linear fit over the observed spectral range (450–950 nm) for the SMOCC experiment data (Pasture Dry to Wet 2002). Low absorption coefficients are associated with low Ångström exponents.
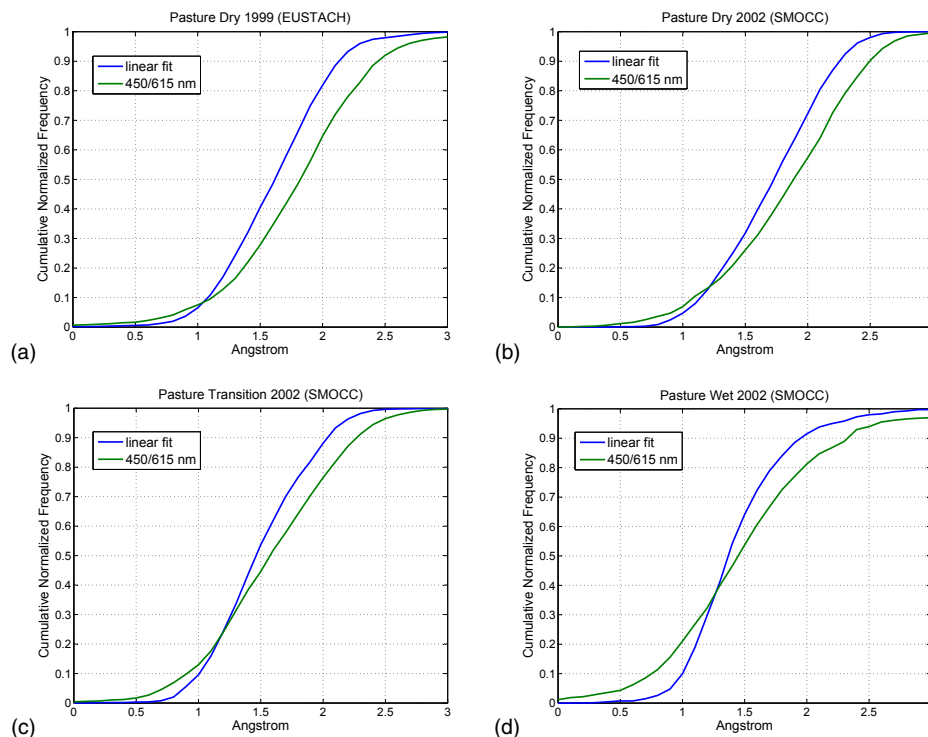
Fig. 5. Cumulative histogram of absorption Ångström exponents for: **(a)** Pasture Dry 1999 (LBA/EUSTACH); **(b)** Pasture Dry 2002; **(c)** Pasture Transition 2002 and **(d)** Pasture Wet 2002 (LBA/SMOCC). Ångström exponents were calculated based on the slope between neighboring wavelengths ($\mathring{a}_{abs}^{450/615}$) and based on linear fits over the whole measured spectrum ($\mathring{a}_{abs}^{lin}$).

Pasture Dry to Wet 2002 (LBA/SMOCC)
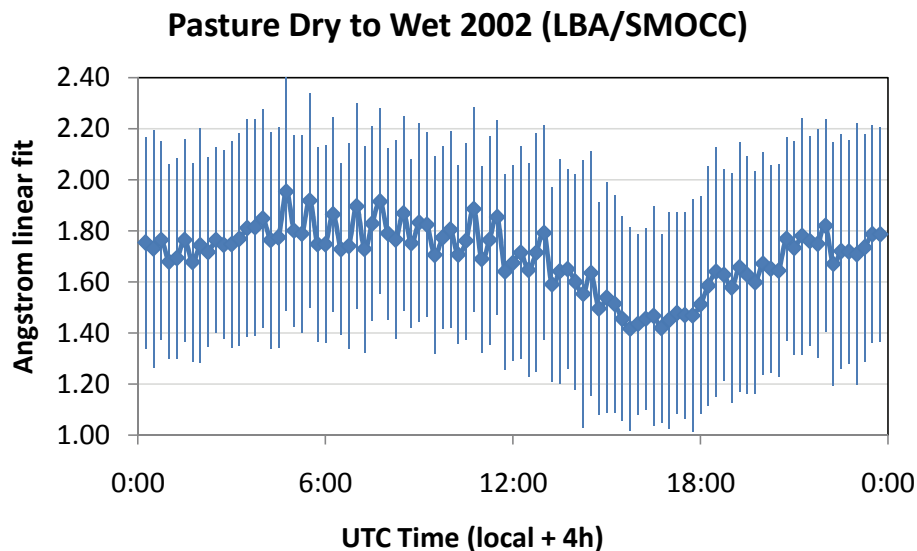
Fig. 6. Average diurnal cycle of the $\mathring{a}_{abs}^{lin}$ Ångström exponents calculated for Pasture Dry to Wet 2002 (SMOCC). Bars represent statistical standard deviations.